

PARAMETER-EFFICIENT GENERATIVE MODELING WITH CONTROLLED VECTOR FIELDS

PEYMAN MORTEZA

ABSTRACT. We introduce a continuous-time generative modeling framework, motivated by the Chow–Rashevskii theorem, that builds expressive flows from a small set of fixed vector fields and learned scalar controls. Instead of learning an unconstrained high-dimensional vector field, our framework constructs the velocity by modulating fixed vector fields with learned scalar control functions. When the fixed fields are bracket-generating, their Lie algebra spans the ambient space, providing a mechanism for expressive transport with only a small number of learned control channels and offering a parameter-efficient geometric alternative to standard vector-field parameterizations. This decoupled formulation yields a structured and interpretable generative model in which the number of learned scalar output channels can be chosen independently of the ambient dimension. We formulate an expressivity principle showing that, under suitable controllability and well-posedness assumptions, such controlled flows can transport a source distribution to a target distribution. We train the resulting model using a continuous-normalizing-flow likelihood objective and present proof-of-concept experiments on synthetic distributions.

CONTENTS

1. Introduction	1
2. Preliminaries	2
3. ChowFlow	3
4. Experiments	9
5. Proofs	11
6. Experimental Details	17
References	20

1. INTRODUCTION

Generative models form a cornerstone of modern machine learning and AI, driving advances in areas such as image synthesis, language modeling, and structured data generation (BMR⁺20, HJA20). Among the most successful approaches are flow-based and diffusion models, which have shown remarkable capability in capturing complex, high-dimensional data distributions (DSDB16, SSDK⁺20, PNR⁺21, LCBH⁺22).

In this note, we investigate a continuous-time generative modeling framework that builds expressive flows from a small set of fixed vector fields and learned scalar controls. The key idea is to replace an unconstrained high-dimensional velocity field with a controlled dynamical system whose underlying vector fields are fixed and whose scalar

coefficients are learned. Unlike conventional flow-based models that directly learn high-dimensional vector-valued fields, our approach learns only scalar coefficients over predefined geometric directions (see Lemma 8). Leveraging the Chow–Rashevskii theorem, we formulate an expressivity principle showing that, under suitable admissibility, controllability, and well-posedness assumptions, such controlled flows can transport a source distribution to a target distribution (see Corollary 7), even when restricted to a limited number of control directions.

Intuitively, the Lie algebra generated by the fixed vector fields spans the full tangent space, enabling the system to reach any state through compositions of a few base directions. This results in a compact, parameter-efficient, and structurally interpretable generative framework: the fixed vector fields provide the underlying geometric structure, while the learned scalar controls modulate the dynamics with a small number of output channels. By structural interpretability, we mean that the generative process is explicitly constructed from a fixed, known set of vector fields, while the learned scalar control functions modulate these directions over time. We instantiate the framework with lightweight MLPs that parameterize the scalar control functions (see Algorithm 1) and evaluate its performance on standard synthetic density benchmarks.

The remainder of this note is organized as follows. Section 2 recalls the necessary preliminaries on Lie brackets, the Chow–Rashevskii theorem, and control systems. Section 3 introduces the ChowFlow framework, which replaces unconstrained vector-field parameterizations with learned scalar controls over fixed vector fields satisfying a bracket-generating condition. Section 4 presents proof-of-concept experiments on synthetic distributions. Section 5 provides detailed proofs of the theoretical results, and Section 6 provides additional experimental details.

2. PRELIMINARIES

We provide a brief overview of Lie brackets, the Chow–Rashevskii theorem, and control systems. Detailed expositions can be found in standard references, e.g., (War83, Jur97, Mon02).

Definition 1 (Lie Bracket). *The Lie bracket of two smooth vector fields X and Y on a smooth manifold M , denoted $[X, Y]$, is a smooth vector field defined by,*

$$[X, Y](f) = X(Y(f)) - Y(X(f)),$$

for any smooth function $f : M \rightarrow \mathbb{R}$, where $X(f)$ and $Y(f)$ denote the action of the vector fields on f .

Definition 2 (Left-Invariant Vector Field). *Let G be a Lie group, and let $L_g : G \rightarrow G$ denote left multiplication by $g \in G$, i.e., $L_g(h) = gh$. A smooth vector field $X \in \mathfrak{X}(G)$ is called left-invariant if it is preserved under all left translations,*

$$(dL_g)_h(X(h)) = X(gh), \quad \text{for all } g, h \in G.$$

Equivalently, X is completely determined by its value at the identity element $e \in G$, and extended to all of G by left translation,

$$X(g) = (dL_g)_e(X(e)).$$

The space of left-invariant vector fields is naturally identified with the Lie algebra $T_e G$ of G .

Definition 3 (Control System). A control system on a smooth manifold M is a dynamical system of the form,

$$\dot{x}(t) = \sum_{i=1}^k u_i(t, x(t)) X_i(x(t)),$$

where $\{X_1, X_2, \dots, X_k\}$ are smooth vector fields on M , and $u_i : [0, T] \times M \rightarrow \mathbb{R}$, $1 \leq i \leq k$, are scalar control inputs, or feedback control laws, depending on time and state. Here, k denotes the number of control channels. When classical ODE solutions are considered, we assume the u_i are sufficiently regular to ensure well-posedness.

Theorem 4 (Chow–Rashevskii Theorem (Cho40, Ras38)). Let M be a connected smooth manifold, and let $\Delta = \text{span}\{X_1, \dots, X_k\}$ be a distribution generated by smooth vector fields. If the Lie algebra generated by $\{X_1, \dots, X_k\}$ spans the entire tangent space $T_x M$ at every $x \in M$, i.e.,

$$\text{Lie}\{X_1, \dots, X_k\}(x) = T_x M \quad \forall x \in M,$$

then any two points $p, q \in M$ can be connected by a piecewise smooth, absolutely continuous curve $\gamma : [0, 1] \rightarrow M$ satisfying,

$$\gamma(0) = p, \quad \gamma(1) = q, \quad \dot{\gamma}(t) \in \Delta_{\gamma(t)},$$

for almost every $t \in [0, 1]$.

Remark 1 (Control-theoretic interpretation). The Chow–Rashevskii theorem can be interpreted as a controllability statement: when the vector fields X_1, \dots, X_k are bracket-generating, admissible curves tangent to their span can connect any two points in the same connected component of M . In our setting, this motivates the use of a small set of fixed bracket-generating vector fields as a geometric basis for constructing continuous-time generative flows.

3. CHOWFLOW

In this section, we show how the Chow–Rashevskii theorem motivates a parameter-efficient class of structured continuous-time generative models. Our key observation is that viewing generative flows through the lens of the Chow–Rashevskii theorem leads to a parameter-efficient velocity parameterization: rather than outputting a full d -dimensional vector field, the model learns scalar controls over a small set of fixed bracket-generating vector fields. Specifically, expressive generative behavior can be achieved using only a small number of scalar control functions, provided that the underlying vector fields are appropriately chosen and satisfy the bracket-generating condition of Theorem 4. This perspective offers a structured way to steer the generative process through a low-dimensional set of learnable coefficients, effectively reusing a shared geometric backbone to produce complex transformations. This formulation motivates the construction presented in Algorithm 1.

3.1. Geometric Control and Controlled Flows. We begin by establishing the mathematical foundations of the framework. As stated in Theorem 4, under mild regularity conditions, a suitable control system can steer any initial point to an arbitrary target point. Let μ_0 and μ_1 be two probability measures on (M, g) , and let $\pi \in \Pi(\mu_0, \mu_1)$ be a coupling between them.

Definition 5 (Class of path bridges). *Let \mathcal{F} be a class of absolutely continuous curves $\gamma : [0, 1] \rightarrow M$. We say that \mathcal{F} is a class of path bridges if it satisfies the following properties:*

- (1) **Endpoint connectivity:** *for every pair $(x_0, x_1) \in M \times M$, there exists a path $\gamma^{x_0, x_1} \in \mathcal{F}$ such that $\gamma^{x_0, x_1}(0) = x_0, \gamma^{x_0, x_1}(1) = x_1$.*
- (2) **Measurable selection:** *there exists a measurable map,*

$$\begin{aligned} \Gamma : M \times M &\rightarrow \mathcal{F}, \\ (x_0, x_1) &\mapsto \gamma^{x_0, x_1}, \end{aligned}$$

such that for every $(x_0, x_1) \in M \times M$, the selected path $\gamma^{x_0, x_1} : [0, 1] \rightarrow M$ belongs to \mathcal{F} and satisfies $\gamma^{x_0, x_1}(0) = x_0, \gamma^{x_0, x_1}(1) = x_1$, where \mathcal{F} is understood with its natural measurable structure as a class of paths.

Remark 2. *Let (M, g) be a Riemannian manifold, and let $X_1, \dots, X_k \in \mathfrak{X}(M)$ be smooth vector fields satisfying the Chow–Rashevskii bracket-generating condition, as in Theorem 4. Then the Chow–Rashevskii theorem gives rise to a natural class of path bridges associated with X_1, \dots, X_k . Namely, one may take \mathcal{F} to be the class of absolutely continuous curves $\gamma : [0, 1] \rightarrow M$ such that,*

$$\dot{\gamma}(t) \in \text{span}\{X_1(\gamma(t)), \dots, X_k(\gamma(t))\},$$

for almost every $t \in [0, 1]$. Under the bracket-generating assumption, any two points in the same connected component of M can be connected by a curve in \mathcal{F} .

Remark 3 (Random interpolating path). *Given a class of path-bridges \mathcal{F} , we can construct a random interpolation path between μ_0 and μ_1 . Let (Z_0, Z_1) be a random pair with law π , and define the random path, $Z_t := \gamma_t^{Z_0, Z_1} = \Gamma(Z_0, Z_1)(t), t \in [0, 1]$. For each $t \in [0, 1]$, let μ_t denote the law of Z_t : $\mu_t := \text{Law}(Z_t)$. By construction, $\mu_t = (\text{ev}_t \circ \Gamma)_{\#} \pi$, where $\text{ev}_t(\gamma) = \gamma(t)$ is the evaluation map at time t . In particular, $\mu_0 = \text{Law}(Z_0), \mu_1 = \text{Law}(Z_1)$, so the family $(\mu_t)_{t \in [0, 1]}$ is an interpolation between μ_0 and μ_1 .*

The following bridge-to-velocity construction is inspired by the flow-matching viewpoint (LCBH⁺22): a random family of bridges induces an Eulerian velocity field through conditional averaging. More precisely, given a class of path bridges \mathcal{F} , let (Z_0, Z_1) be a random pair with law π , and define the random path,

$$Z_t := \gamma_t^{Z_0, Z_1} = \Gamma(Z_0, Z_1)(t), \quad t \in [0, 1].$$

The associated Eulerian velocity field is defined by,

$$v_t(x) = \mathbb{E} \left[\dot{\gamma}_t^{Z_0, Z_1} \mid \gamma_t^{Z_0, Z_1} = x \right].$$

When the path bridges are associated to a bracket-generating control system (See Remark 2), the resulting Eulerian velocity admits a feedback-control representation. Related flow-matching and continuity-equation formulations for control-affine systems have been studied in (Ela25, CV25). We use this viewpoint to motivate the controlled-flow parameterization below.

Theorem 6. *Let μ_0 and μ_1 be probability measures on (M, g) , and let $\pi \in \Pi(\mu_0, \mu_1)$ be a coupling. Let \mathcal{F} be a class of path bridges as in Definition 5. Let (Z_0, Z_1) be a random pair with law π , and define the random path $Z_t := \gamma_t^{Z_0, Z_1}, t \in [0, 1]$ (See Remark 3). Let $\mu_t := \text{Law}(Z_t)$, and $v_t(x) = \mathbb{E}[\dot{\gamma}_t^{Z_0, Z_1} \mid \gamma_t^{Z_0, Z_1} = x]$. Under standard integrability/regularity assumptions (see Section 5 for details), the following statements hold.*

(i) *The pair (μ_t, v_t) satisfies the continuity equation $\partial_t \mu_t + \text{div}_g(\mu_t v_t) = 0$ in the weak sense, that is, for every $\varphi \in C_c^\infty(M)$ and for almost every $t \in [0, 1]$,*

$$\frac{d}{dt} \int_M \varphi(x) d\mu_t(x) = \int_M d\varphi(v_t(x)) d\mu_t(x) = \int_M g_x(\nabla_g \varphi(x), v_t(x)) d\mu_t(x).$$

(ii) *Consider the ODE,*

$$\begin{aligned} \dot{Y}_t &= v_t(Y_t), \\ Y_0 &= y, \end{aligned}$$

Assume that the time-dependent vector field v_t is regular enough to generate a unique non-autonomous flow map $\phi_{0,t}$, and that the associated continuity equation is uniquely solved by the corresponding flow pushforward. For simplicity, write $\phi_t := \phi_{0,t}$, then,

$$\mu_t = (\phi_t)_\# \mu_0 \quad \text{for all } t \in [0, 1].$$

In particular, $(\phi_1)_\# \mu_0 = \mu_1$.

The next corollary specializes the preceding bridge-to-velocity construction to admissible bridges generated by a bracket-generating control system.

Corollary 7 (Pushforward of Distributions via Controlled Flows). *Let (M, g) be a Riemannian manifold, and let $X_1, \dots, X_k \in \mathfrak{X}(M)$ be smooth vector fields satisfying the Chow–Rashevskii bracket-generating condition. Assume that the hypotheses of Theorem 6 hold for the class of path bridges associated with X_1, \dots, X_k . There exist measurable feedback control laws $u_i(t, x)$, $1 \leq i \leq k$, such that the associated dynamical system,*

$$\dot{x}(t) = \sum_{i=1}^k u_i(t, x(t)) X_i(x(t)),$$

generates a flow ϕ_t satisfying,

$$(\phi_1)_\# \mu_0 = \mu_1.$$

In particular, the initial measure μ_0 can be transported to the target measure μ_1 by feedback controls depending only on (t, x) , rather than explicitly on the initial point.

To operationalize this framework, we seek a set of vector fields whose cardinality is independent of the ambient dimension but still satisfies the bracket-generating condition in Theorem 4. The following lemma shows that in \mathbb{R}^d , just two appropriately chosen vector fields suffice to generate the entire tangent space. Combined with Corollary 7, this result enables the design of expressive generative models using only two scalar control functions.

Lemma 8. *On \mathbb{R}^d (with coordinates x_1, \dots, x_d), $d \geq 3$, define the vector fields,*

$$V_1 = \frac{\partial}{\partial x_1} + x_2 \frac{\partial}{\partial x_3} + x_3 \frac{\partial}{\partial x_4} + \dots + x_{d-1} \frac{\partial}{\partial x_d}, \quad V_2 = \frac{\partial}{\partial x_2}.$$

Then the Lie algebra generated by V_1 and V_2 spans the tangent space $T_x \mathbb{R}^d$ at every point $x \in \mathbb{R}^d$.

Proof. The proof is provided in Section 5. □

Remark 4 (Coordinate permutations). *The construction in Lemma 8 is not tied to the particular ordering (x_1, \dots, x_d) . For any permutation (i_1, \dots, i_d) of the coordinate indices, the pair,*

$$V_1 = \partial_{x_{i_1}} + x_{i_2} \partial_{x_{i_3}} + \dots + x_{i_{d-1}} \partial_{x_{i_d}}, \quad V_2 = \partial_{x_{i_2}}$$

is also bracket-generating. This follows either by repeating the bracket calculation or by observing that bracket generation is invariant under coordinate permutations.

Remark 5. *Under the assumptions of Corollary 7, Lemma 8 shows that two appropriately chosen vector fields are sufficient to obtain a bracket-generating structure in \mathbb{R}^d . This generalizes classical flow-based generative models (CRBD18, PNR⁺21, LCBH⁺22), where $M = \mathbb{R}^d$ and the vector fields are taken to be the standard basis $X_i = \frac{\partial}{\partial x_i}$. In contrast, our framework allows for a much smaller set of vector fields, provided they generate the full tangent space via Lie brackets. This flexibility is the core insight behind our parameter-efficient approach.*

Remark 6 (Parameter efficiency). *Lemma 8 shows that, in principle, two appropriately chosen vector fields can bracket-generate the full tangent space in arbitrary ambient dimension d . Consequently, the number of learned scalar control channels can be kept fixed at $k = 2$, independently of d . This should be contrasted with standard continuous-time flow parameterizations, where the model typically outputs a full d -dimensional velocity vector. In that case, the number of output channels scales linearly with the ambient dimension. In our formulation, the network only outputs the scalar controls multiplying the fixed vector fields. Thus, when each control channel is modeled by a neural network of comparable size, the bracket-generating construction can substantially reduce the number of learned output channels while retaining expressivity through Lie-bracket generation. This statement concerns the number of scalar output channels; the total number of neural-network parameters may still depend on the ambient dimension through the input layer and hidden representation.*

To illustrate how Lemma 8 operates in low dimensions, we consider the Heisenberg group, a canonical example in geometric control theory that demonstrates how Lie brackets enable access to new directions beyond the original vector fields.

Example 9 (Heisenberg Group). *The (first) Heisenberg group \mathbb{H} is the manifold \mathbb{R}^3 equipped with the group law,*

$$(x_1, x_2, x_3) \cdot (y_1, y_2, y_3) = (x_1 + y_1, x_2 + y_2, x_3 + y_3 + x_1 y_2).$$

A standard horizontal generating pair of left-invariant vector fields is,

$$V_2 = \frac{\partial}{\partial x_2} + x_1 \frac{\partial}{\partial x_3}, \quad V_1 = \frac{\partial}{\partial x_1}.$$

These fields satisfy,

$$[V_1, V_2] = \frac{\partial}{\partial x_3},$$

and together $\{V_1, V_2, [V_1, V_2]\}$ span the full tangent space $T_x \mathbb{R}^3$ at every point.

3.2. Learning Distribution Flows via Control Vector Fields. Building on Lemma 8, we introduce a CNF-style generative modeling algorithm that transports a simple source distribution μ_0 (e.g., a standard Gaussian) to a target data distribution μ_1 through a controlled continuous-time flow. The central idea is to replace an unconstrained full-dimensional vector field by a structured control-weighted combination of fixed geometric vector fields with learned scalar coefficients. Thus, instead of directly learning an arbitrary velocity field $v_\theta(t, x) \in \mathbb{R}^d$, we parameterize it as,

$$v_\theta(t, x) = \sum_{i=1}^k a_i(t, x; \theta) V_i(x),$$

where V_1, \dots, V_k are fixed vector fields and $a_i(t, x; \theta)$ are scalar control functions. When the V_i satisfy the bracket-generating condition of Theorem 4, the resulting system retains strong controllability properties while using only a small number of learned scalar control channels. In the Euclidean setting, we use the explicit construction from Lemma 8. Namely, we define,

$$V_1 = \frac{\partial}{\partial x_1} + x_2 \frac{\partial}{\partial x_3} + \dots + x_{d-1} \frac{\partial}{\partial x_d}, \quad V_i = \frac{\partial}{\partial x_i}, \quad 2 \leq i \leq k.$$

For $k = 2$, Lemma 8 shows that V_1, V_2 already bracket-generate $T\mathbb{R}^d$. More generally, one may choose $k \geq 2$ fixed vector fields satisfying the same bracket-generating condition.

3.3. Parameterization. Each scalar control a_i is implemented as a neural network with input $(t, x) \in [0, T] \times \mathbb{R}^d$ and scalar output. This is a Markovian parameterization: unlike the endpoint-matching formulation, the controls do not explicitly depend on the initial point x_0 . This choice allows the model to define a standard continuous-time flow and to be trained by likelihood using the continuous normalizing flow change-of-variables formula.

3.4. Dynamics. The learned flow is defined by the ODE,

$$\dot{x}(t) = v_\theta(t, x(t)) = \sum_{i=1}^k a_i(t, x(t); \theta) V_i(x(t)).$$

Algorithm 1 CNF-style ChowFlow Training in \mathbb{R}^d

- 1: **Input:** number of control fields $2 \leq k \leq d$, dimension $d \geq 3$; samples $\{y^{(i)}\}_{i=1}^N \sim \mu_1$, base distribution μ_0 with density p_0 , terminal time $T = 1$, number of ODE steps K .
- 2: **Output:** Trained scalar controls $a_i(t, x; \theta)$, $1 \leq i \leq k$.
- 3: Initialize $a_i(\cdot; \theta_i)$ as MLPs with input (t, x) , $1 \leq i \leq k$.
- 4: $V_1 \leftarrow \partial_{x_1} + x_2 \partial_{x_3} + \dots + x_{d-1} \partial_{x_d}$.
- 5: $V_i \leftarrow \partial_{x_i}$ for $2 \leq i \leq k$.
- 6: Define the velocity field,

$$v_\theta(t, x) := \sum_{i=1}^k a_i(t, x; \theta) V_i(x).$$

- 7: **while** not converged **do**
- 8: Sample minibatch $\{y^{(j)}\}_{j=1}^B \sim \mu_1$
- 9: **for** each $y^{(j)}$ **do**
- 10: Integrate the dynamics backward from $t = T$ to $t = 0$ using K ODE steps, while accumulating the divergence:

$$\frac{dX_t^{(j)}}{dt} = v_\theta(t, X_t^{(j)}), \quad X_T^{(j)} = y^{(j)}.$$

- 11: Let $z^{(j)} := X_0^{(j)}$ and,

$$\Delta^{(j)} := \int_0^T \operatorname{div}(v_\theta(t, X_t^{(j)})) dt.$$

- 12: Compute:

$$\log p_\theta(y^{(j)}) = \log p_0(z^{(j)}) - \Delta^{(j)}.$$

- 13: **end for**
- 14: Minimize the negative log-likelihood,

$$\mathcal{L}_{\text{CNF}}(\theta) = -\frac{1}{B} \sum_{j=1}^B \log p_\theta(y^{(j)}).$$

- 15: Update θ by backpropagation through the ODE solver.
 - 16: **end while**
 - 17: **return** trained controls $a_i(t, x; \theta)$
-

When $V_i = \partial_{x_i}$ for $i = 1, \dots, d$, this reduces to the usual continuous normalizing flow parameterization,

$$v_\theta(t, x) = (a_1(t, x; \theta), \dots, a_d(t, x; \theta)).$$

3.5. Likelihood training. Let p_0 denote the density of the base distribution μ_0 , for example p_0 may be the density of a standard Gaussian distribution. The density p_t induced by the ODE satisfies the continuity equation,

$$\partial_t p_t + \operatorname{div}((p_t v_\theta)) = 0.$$

Equivalently, along a trajectory x_t solving $\dot{x}_t = v_\theta(t, x_t)$, the log-density evolves according to,

$$\frac{d}{dt} \log p_t(x_t) = -\operatorname{div}(v_\theta(t, x_t)).$$

Thus, for a data sample $x_T \sim \mu_1$, we integrate the dynamics backward from $t = T$ to $t = 0$, while accumulating the divergence correction:

$$\frac{dx_t}{dt} = v_\theta(t, x_t), \quad x_T = x_{\text{data}},$$

If the backward integration gives $z = x_0$ and,

$$\Delta = \int_0^T \operatorname{div}(v_\theta(t, x_t)) dt,$$

then the model likelihood is computed by,

$$\log p_\theta(x_{\text{data}}) = \log p_0(z) - \Delta.$$

The training objective is the negative log-likelihood,

$$\mathcal{L}_{\text{CNF}}(\theta) = -\mathbb{E}_{x \sim \mu_1} [\log p_\theta(x)].$$

3.6. Optimization. In practice, the augmented ODE is solved numerically, and the divergence $\operatorname{div}(v_\theta)$ is computed either exactly by automatic differentiation or approximately using a trace estimator in high dimensions. The parameters θ of the scalar control networks are trained by backpropagation through the ODE solver. Algorithm 1 summarizes the resulting CNF-style ChowFlow training procedure.

4. EXPERIMENTS

In this section, we evaluate the proposed framework through a series of experiments. We begin by demonstrating that our framework enables parameter-efficient generative modeling on several standard synthetic benchmarks. In particular, we consider three-dimensional settings where the underlying control system is governed by two vector fields constructed as in Lemma 8.

4.1. Simulation Setup. In synthetic experiments, the source distribution μ_0 is a standard Gaussian in \mathbb{R}^3 , i.e., $\mu_0 = \mathcal{N}(0, I)$. The target distribution μ_1 varies across tasks and includes several challenging benchmarks commonly used to evaluate flow-based models: (1) a two-moons distribution embedded in three dimensions, (2) a nonlinearly embedded torus (ring), and (3) a mixture of well-separated Gaussians. These targets exhibit either multimodality or complex geometry, making them nontrivial to model.

The system dynamics are defined by two fixed, smooth vector fields V_1 and V_2 (as described in Lemma 8), while the scalar control functions $a_1(t, x)$ and $a_2(t, x)$ are parameterized by small MLPs. Training is performed by maximum likelihood using the continuous normalizing flow change-of-variables formula. Specifically, we integrate data samples backward through the learned controlled dynamics to the Gaussian base distribution while accumulating the divergence term of the induced vector field. Additional training and hyperparameter details are provided in Section 6.

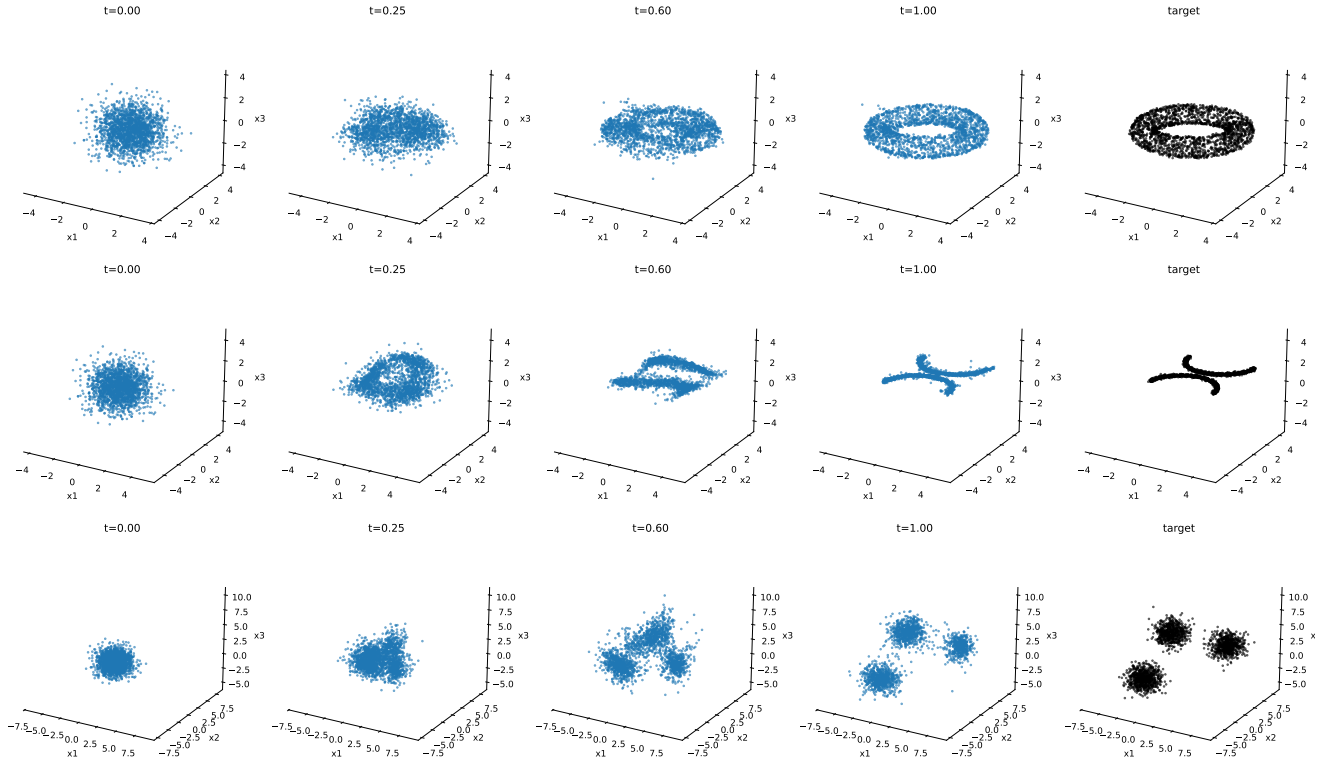


FIGURE 1. Algorithm 1 applied to 3D synthetic distributions. Each row illustrates the learned transport from a simple Gaussian base distribution (left) to a complex target distribution (right). The target samples, shown in black, include a torus, two moons, and a Gaussian mixture. Intermediate transported samples are shown in blue. The flow qualitatively captures the geometric structure of the target using only two control channels (as constructed in Lemma 8), despite the ambient dimension being three.

4.2. Visualization of Learned Transport. Figure 1 illustrates the transport induced by Algorithm 1 on several synthetic distributions in \mathbb{R}^3 , including a mixture of Gaussians, a two-moons manifold embedded in 3D, and a nonlinear torus-like structure. In each row, we visualize three key stages: (1) the initial samples drawn from a simple Gaussian prior (left), (2) intermediate samples during transport (middle, shown in blue), and (3) final transported samples (right). The target samples are visualized in black for reference.

Despite using only two control channels, the learned flows qualitatively match the geometric structure of each target. In the Gaussian mixture case, the model separates and places mass near the correct modes. In the two-moons case, the flow deforms the isotropic prior into a curved bimodal support. For the torus, the learned flow captures the ring-like geometry without collapsing or overshooting. These results highlight the expressiveness of the proposed framework in low-dimensional settings. They also provide a geometric intuition for how our framework leverages the bracket structure of its vector fields to construct complex transformations with minimal parameterization.

5. PROOFS

In this section, we provide detailed proofs of the theoretical results stated above. We begin with Lemma 8.

Lemma (Restatement of Lemma 8). *On \mathbb{R}^d (with coordinates x_1, \dots, x_d), $d \geq 3$, define the vector fields*

$$V_1 = \frac{\partial}{\partial x_1} + x_2 \frac{\partial}{\partial x_3} + x_3 \frac{\partial}{\partial x_4} + \dots + x_{d-1} \frac{\partial}{\partial x_d}, \quad V_2 = \frac{\partial}{\partial x_2}.$$

Then the Lie algebra generated by V_1 and V_2 spans the tangent space $T_x \mathbb{R}^d$ at every point $x \in \mathbb{R}^d$.

Proof. First, we compute the commutator:

$$[V_1, V_2] = V_1 V_2 - V_2 V_1.$$

Since $V_2 = \frac{\partial}{\partial x_2}$, only the term in V_1 involving x_2 contributes. Thus,

$$[V_1, V_2] = -\frac{\partial}{\partial x_3}.$$

We now claim that for $k = 1, \dots, d-2$,

$$\text{ad}_{V_1}^k(V_2) := [V_1, [V_1, \dots, [V_1, V_2] \dots]] = (-1)^k \frac{\partial}{\partial x_{k+2}}.$$

We prove this by induction on k . For the base case $k = 1$, we have already shown $[V_1, V_2] = -\frac{\partial}{\partial x_3}$. Suppose that for some $k \geq 1$,

$$\text{ad}_{V_1}^k(V_2) = (-1)^k \frac{\partial}{\partial x_{k+2}}.$$

Then,

$$[V_1, \frac{\partial}{\partial x_{k+2}}]$$

acts nontrivially only on the term $x_{k+2} \frac{\partial}{\partial x_{k+3}}$ in V_1 , whose derivative with respect to x_{k+2} is exactly $\frac{\partial}{\partial x_{k+3}}$. Therefore,

$$[V_1, \frac{\partial}{\partial x_{k+2}}] = -\frac{\partial}{\partial x_{k+3}}.$$

By induction, the Lie algebra generated by V_1 and V_2 contains $\frac{\partial}{\partial x_i}$ for all $i = 2, \dots, d$ up to sign. In particular, for any $x = (x_1, \dots, x_d) \in \mathbb{R}^d$, we have $\frac{\partial}{\partial x_i}$ for $2 \leq i \leq d$ in $T_x \mathbb{R}^d$. Together with V_1 , the collection $\{V_1, \frac{\partial}{\partial x_2}, \dots, \frac{\partial}{\partial x_d}\}$ spans $T_x \mathbb{R}^d$ at every point x . Thus, the conditions of Theorem 4 are satisfied. \square

Example 10 (Relation of Lemma 8 to Heisenberg Group). *Consider the case $d = 3$, so that our space is \mathbb{R}^3 with coordinates (x_1, x_2, x_3) . Define the vector fields,*

$$V_2 = \frac{\partial}{\partial x_2} + x_1 \frac{\partial}{\partial x_3}, \quad V_1 = \frac{\partial}{\partial x_1}.$$

These are precisely the standard generating vector fields for the (first) Heisenberg group \mathbb{H} . To see that V_1 and V_2 generate the entire tangent space at each point, compute their commutator:

$$[V_1, V_2] = \frac{\partial}{\partial x_3},$$

Therefore, the Lie algebra generated by V_1 and V_2 contains the full set $\left\{ \frac{\partial}{\partial x_1}, \frac{\partial}{\partial x_2}, \frac{\partial}{\partial x_3} \right\}$ at every point. This is analogous to the structure described in Lemma 8, up to a permutation of coordinates.

Next, we restate and prove Theorem 6. Let μ_0 and μ_1 be probability measures on (M, g) , and let $\pi \in \Pi(\mu_0, \mu_1)$ be a coupling between them. We impose the following integrability and regularity assumptions. The integrability assumptions justify the use of the chain rule along the random paths and the interchange of expectation and time integration. The regularity assumption ensures that the Eulerian velocity field induced by conditional averaging generates a unique well-posed flow. Throughout the following, we assume that,

(1)

$$\mathbb{E} \int_0^1 \left\| \dot{Z}_t \right\|_g dt < \infty;$$

(2) there exists a Borel vector field,

$$v : [0, 1] \times M \rightarrow TM, \quad v_t(x) \in T_x M,$$

such that,

$$v_t(Z_t) = \mathbb{E}[\dot{Z}_t \mid Z_t]$$

almost surely for almost every $t \in [0, 1]$. Assume in addition that the induced velocity field v is regular enough to generate a unique global flow. For example, when M is compact, the condition,

$$v \in L^1([0, 1]; C^1(M; TM)),$$

is sufficient to generate a unique non-autonomous flow and to ensure that the continuity equation is uniquely solved by the corresponding flow pushforward.

Under these assumptions, the field v_t transports the interpolating marginals (μ_t) in the sense of the continuity equation.

Theorem (Restatement of Theorem 6). *Let μ_0 and μ_1 be probability measures on (M, g) , and let $\pi \in \Pi(\mu_0, \mu_1)$ be a coupling. Let \mathcal{F} be a class of path bridges as in Definition 5. Let (Z_0, Z_1) be a random pair with law π , and define the random path $Z_t := \gamma_t^{Z_0, Z_1}$, $t \in [0, 1]$ (See Remark 3). Let $\mu_t := \text{Law}(Z_t)$, and $v_t(x) = \mathbb{E}[\dot{\gamma}_t^{Z_0, Z_1} \mid \gamma_t^{Z_0, Z_1} = x]$. Under the above assumptions, the following statements hold.*

(i) *The pair (μ_t, v_t) satisfies the continuity equation $\partial_t \mu_t + \text{div}_g(\mu_t v_t) = 0$ in the weak sense, that is, for every $\varphi \in C_c^\infty(M)$ and for almost every $t \in [0, 1]$,*

$$\frac{d}{dt} \int_M \varphi(x) d\mu_t(x) = \int_M d\varphi(v_t(x)) d\mu_t(x) = \int_M g_x(\nabla_g \varphi(x), v_t(x)) d\mu_t(x).$$

(ii) Consider the ODE,

$$\begin{aligned}\dot{Y}_t &= v_t(Y_t), \\ Y_0 &= y,\end{aligned}$$

Assume that the time-dependent vector field v_t is regular enough to generate a unique non-autonomous flow map $\phi_{0,t}$, and that the associated continuity equation is uniquely solved by the corresponding flow pushforward. For simplicity, write $\phi_t := \phi_{0,t}$, then,

$$\mu_t = (\phi_t)_\# \mu_0 \quad \text{for all } t \in [0, 1].$$

In particular, $(\phi_1)_\# \mu_0 = \mu_1$.

Proof. (i) Fix $\varphi \in C_c^\infty(M)$. Since $t \mapsto Z_t$ is absolutely continuous for almost every realization, the chain rule yields,

$$\frac{d}{dt} \varphi(Z_t) = g(\nabla_g \varphi(Z_t), \dot{Z}_t),$$

for almost every $t \in [0, 1]$ and almost surely. Because $\varphi \in C_c^\infty(M)$, its Riemannian gradient is bounded, $\|\nabla_g \varphi\|_{L^\infty} < \infty$. Hence, by Cauchy–Schwarz,

$$\left| g_{Z_t}(\nabla_g \varphi(Z_t), \dot{Z}_t) \right| \leq \|\nabla_g \varphi\|_{L^\infty} \left\| \dot{Z}_t \right\|_g.$$

By the assumption,

$$\mathbb{E} \int_0^1 \left\| \dot{Z}_t \right\|_g dt < \infty,$$

we obtain,

$$\mathbb{E} \int_0^1 \left| g_{Z_t}(\nabla_g \varphi(Z_t), \dot{Z}_t) \right| dt < \infty.$$

Consequently, by the fundamental theorem of calculus for absolutely continuous functions,

$$\frac{d}{dt} \mathbb{E}[\varphi(Z_t)] = \mathbb{E} \left[g_{Z_t}(\nabla_g \varphi(Z_t), \dot{Z}_t) \right],$$

for almost every $t \in [0, 1]$. Since Z_t has law μ_t , we have,

$$\mathbb{E}[\varphi(Z_t)] = \int_M \varphi(x) d\mu_t(x).$$

Consequently,

$$\frac{d}{dt} \int_M \varphi(x) d\mu_t(x) = \mathbb{E} \left[g_{Z_t}(\nabla_g \varphi(Z_t), \dot{Z}_t) \right].$$

Next, we rewrite the right-hand side as an Eulerian integral depending only on the current position Z_t . Since $\nabla_g \varphi(Z_t)$ is measurable with respect to the sigma-algebra generated by Z_t , the defining property of conditional expectation gives,

$$\mathbb{E} \left[g_{Z_t}(\nabla_g \varphi(Z_t), \dot{Z}_t) \right] = \mathbb{E} \left[g_{Z_t}(\nabla_g \varphi(Z_t), \mathbb{E}[\dot{Z}_t \mid Z_t]) \right].$$

By definition,

$$\mathbb{E}[\dot{Z}_t \mid Z_t] = v_t(Z_t),$$

almost surely. Therefore,

$$\mathbb{E} \left[g_{Z_t}(\nabla_g \varphi(Z_t), \dot{Z}_t) \right] = \mathbb{E} \left[g_{Z_t}(\nabla_g \varphi(Z_t), v_t(Z_t)) \right].$$

Using again that $Z_t \sim \mu_t$, this becomes,

$$\mathbb{E} \left[g_{Z_t}(\nabla_g \varphi(Z_t), v_t(Z_t)) \right] = \int_M g_x(\nabla_g \varphi(x), v_t(x)) d\mu_t(x).$$

Combining the identities above, we obtain, for every $\varphi \in C_c^\infty(M)$ and for almost every $t \in [0, 1]$,

$$\frac{d}{dt} \int_M \varphi(x) d\mu_t(x) = \int_M g_x(\nabla_g \varphi(x), v_t(x)) d\mu_t(x).$$

Since the Riemannian gradient $\nabla_g \varphi$ is characterized by,

$$d\varphi_x(w) = g_x(\nabla_g \varphi(x), w), \quad w \in T_x M,$$

the right-hand side can equivalently be written as,

$$\int_M d\varphi_x(v_t(x)) d\mu_t(x).$$

Thus,

$$\frac{d}{dt} \int_M \varphi d\mu_t = \int_M d\varphi(v_t) d\mu_t.$$

We now identify this identity with the weak formulation of the continuity equation. Formally, if μ_t has a smooth density ρ_t with respect to the Riemannian volume measure $d\text{vol}_g$, so that,

$$d\mu_t = \rho_t d\text{vol}_g,$$

then the Riemannian continuity equation is,

$$\partial_t \rho_t + \text{div}_g(\rho_t v_t) = 0.$$

Multiplying this equation by a test function $\varphi \in C_c^\infty(M)$ and integrating over M , we get,

$$\int_M \varphi \partial_t \rho_t d\text{vol}_g + \int_M \varphi \text{div}_g(\rho_t v_t) d\text{vol}_g = 0.$$

The first term is,

$$\int_M \varphi \partial_t \rho_t d\text{vol}_g = \frac{d}{dt} \int_M \varphi \rho_t d\text{vol}_g = \frac{d}{dt} \int_M \varphi d\mu_t.$$

For the second term, using the Riemannian integration-by-parts formula and the fact that φ has compact support, we obtain,

$$\int_M \varphi \text{div}_g(\rho_t v_t) d\text{vol}_g = - \int_M d\varphi(v_t) \rho_t d\text{vol}_g = - \int_M d\varphi(v_t) d\mu_t.$$

Therefore the weak form becomes,

$$\frac{d}{dt} \int_M \varphi d\mu_t = \int_M d\varphi(v_t) d\mu_t.$$

This is precisely the identity derived above. Hence the curve of measures $(\mu_t)_{t \in [0,1]}$, together with the Eulerian velocity field v_t , satisfies the Riemannian continuity equation,

$$\partial_t \mu_t + \operatorname{div}_g(\mu_t v_t) = 0,$$

in the weak sense.

(ii) Define,

$$\nu_t := (\phi_t)_\# \mu_0.$$

We claim that (ν_t) also satisfies the Riemannian continuity equation with velocity field v_t and initial datum μ_0 . Fix again $\varphi \in C_c^\infty(M)$. By definition of pushforward,

$$\int_M \varphi(x) d\nu_t(x) = \int_M \varphi(\phi_t(y)) d\mu_0(y).$$

Differentiate in t . Since $t \mapsto \phi_t(y)$ solves the ODE,

$$\frac{d}{dt} \phi_t(y) = v_t(\phi_t(y)),$$

the chain rule on the manifold gives,

$$\frac{d}{dt} \varphi(\phi_t(y)) = d\varphi_{\phi_t(y)}(v_t(\phi_t(y))),$$

Under the assumed well-posedness and regularity of the flow, differentiation under the integral sign is justified. Hence, for almost every t ,

$$\frac{d}{dt} \int_M \varphi(x) d\nu_t(x) = \int_M d\varphi_{\phi_t(y)}(v_t(\phi_t(y))) d\mu_0(y).$$

Equivalently, pushing forward by ϕ_t , this becomes,

$$\frac{d}{dt} \int_M \varphi(x) d\nu_t(x) = \int_M d\varphi_x(v_t(x)) d\nu_t(x).$$

Thus (ν_t) is a weak solution of the Riemannian continuity equation,

$$\partial_t \nu_t + \operatorname{div}_g(\nu_t v_t) = 0.$$

At time $t = 0$, since $\phi_0 = \operatorname{Id}$, we have,

$$\nu_0 = (\phi_0)_\# \mu_0 = \mu_0.$$

By part (i), the family (μ_t) is also a weak solution of the same continuity equation with the same initial datum μ_0 . By the assumed uniqueness of weak solutions in the class under consideration, it follows that,

$$\mu_t = \nu_t = (\phi_t)_\# \mu_0 \quad \text{for all } t \in [0, 1].$$

Evaluating at $t = 1$, we obtain,

$$(\phi_1)_\# \mu_0 = \mu_1.$$

Thus the flow ϕ_1 transports μ_0 to μ_1 . This proves part (ii).

□

Corollary (Restatement of Corollary 7). *Let (M, g) be a Riemannian manifold, and let $X_1, \dots, X_k \in \mathfrak{X}(M)$ be smooth vector fields satisfying the Chow–Rashevskii bracket-generating condition. Assume that the hypotheses of Theorem 6 hold for the class of path bridges associated with X_1, \dots, X_k . There exist measurable feedback control laws $u_i(t, x)$, $1 \leq i \leq k$, such that the associated dynamical system,*

$$\dot{x}(t) = \sum_{i=1}^k u_i(t, x(t)) X_i(x(t)),$$

generates a flow ϕ_t satisfying,

$$(\phi_1)_\# \mu_0 = \mu_1.$$

In particular, the initial measure μ_0 can be transported to the target measure μ_1 by feedback controls depending only on (t, x) , rather than explicitly on the initial point.

Proof. Let $(Z_0, Z_1) \sim \pi$, and let,

$$Z_t = \gamma_t^{Z_0, Z_1},$$

be the random admissible bridge associated with the admissible path class generated by X_1, \dots, X_k . Since the bridges are admissible, for almost every $t \in [0, 1]$ there exist measurable pathwise controls,

$$\alpha_i^{Z_0, Z_1}(t), \quad 1 \leq i \leq k,$$

such that,

$$\dot{Z}_t = \sum_{i=1}^k \alpha_i^{Z_0, Z_1}(t) X_i(Z_t).$$

By Theorem 6, the induced Eulerian velocity field is,

$$v_t(x) = \mathbb{E}[\dot{Z}_t \mid Z_t = x].$$

Using the admissible representation of \dot{Z}_t , we obtain,

$$v_t(x) = \mathbb{E} \left[\sum_{i=1}^k \alpha_i^{Z_0, Z_1}(t) X_i(Z_t) \mid Z_t = x \right].$$

Since $X_i(Z_t) = X_i(x)$ after conditioning on $Z_t = x$, this gives,

$$v_t(x) = \sum_{i=1}^k \mathbb{E} \left[\alpha_i^{Z_0, Z_1}(t) \mid Z_t = x \right] X_i(x).$$

Define the feedback controls,

$$u_i(t, x) := \mathbb{E} \left[\alpha_i^{Z_0, Z_1}(t) \mid Z_t = x \right].$$

Then,

$$v_t(x) = \sum_{i=1}^k u_i(t, x) X_i(x).$$

Therefore the ODE,

$$\dot{x}(t) = v_t(x(t)),$$

can be written as the feedback-controlled system,

$$\dot{x}(t) = \sum_{i=1}^k u_i(t, x(t)) X_i(x(t)).$$

By Theorem 6, under the stated regularity assumptions, the time-dependent vector field v_t generates a flow ϕ_t satisfying,

$$\mu_t = (\phi_t)_\# \mu_0.$$

Evaluating at $t = 1$, and using $\mu_1 = \text{Law}(Z_1)$, we obtain,

$$(\phi_1)_\# \mu_0 = \mu_1.$$

Thus the initial measure μ_0 is transported to the target measure μ_1 by feedback controls depending only on (t, x) . \square

6. EXPERIMENTAL DETAILS

This section provides additional details about the synthetic datasets used in the experiments presented in this note.

6.1. 3D Moon Dataset. We construct the synthetic *3D moon* dataset by extending the classic 2D two-moons distribution into three dimensions. The first “moon” lies on the x - y plane as a semicircular arc of unit radius centered at the origin, with $z = 0$. The second “moon” is placed in the parallel plane $z = 1$, translated along the y -axis and horizontally flipped to form a complementary arc. Gaussian noise with standard deviation 0.1 is added to each point to introduce variability. The resulting dataset exhibits a simple yet nontrivial topology in \mathbb{R}^3 , requiring models to capture both geometric structure and local noise.

6.2. Multi-Component Gaussian Mixture. We generate a synthetic multimodal distribution μ_1 in \mathbb{R}^D using a mixture of three anisotropic Gaussian components. Each component is defined by a distinct mean vector in the first three dimensions—specifically, $[6, 3, 3]$, $[-2, -3, -2]$, and $[0, 0, 5]$ —with the remaining dimensions set to zero. Each component uses a fixed covariance vector. The batch is split approximately evenly across components, and samples are generated by scaling standard Gaussian noise with the specified variances and shifting by the corresponding means. The samples are then shuffled to eliminate ordering artifacts. This setup results in a structured, high-dimensional distribution with multiple modes, providing a challenging testbed for generative models.

6.3. 3D Torus Dataset. We construct a synthetic dataset by sampling points from a 3D torus embedded in \mathbb{R}^3 , defined by a major radius $R = 3.0$ and a minor radius $r = 0.75$. For each sample, two angles $\theta, \phi \sim \mathcal{U}(0, 2\pi)$ are drawn, and the point is computed using the parametric equations:

$$x = (R + r \cos \phi) \cos \theta, \quad y = (R + r \cos \phi) \sin \theta, \quad z = r \sin \phi.$$

To simulate realistic conditions, Gaussian noise with standard deviation 0.07 is independently added to each coordinate. The resulting point cloud lies on a tubular manifold, offering a challenging geometry with nontrivial curvature and topology.

6.4. Control parameterization. The scalar controls a_i are parameterized by multi-layer perceptrons. Each scalar control network is an MLP with three hidden layers of width 128 and SiLU activations. We train for 3000 iterations with minibatch size $B = 512$.

6.5. Numerical integration. For the CNF-style experiments, the controls are Markovian functions of time and state, $a_i = a_i(t, x; \theta)$, and the induced velocity field is,

$$v_\theta(t, x) = \sum_{i=1}^k a_i(t, x; \theta) V_i(x).$$

We simulate the dynamics over the time interval $[0, 1]$. During training, for each data sample $x_1 \sim \mu_1$, we integrate the controlled ODE backward from $t = 1$ to $t = 0$,

$$\dot{x}_t = v_\theta(t, x_t), \quad x_{t=1} = x_1.$$

In the implementation, we use a fixed-step Runge–Kutta method with K steps. For sampling, we draw $z \sim p_0 = \mathcal{N}(0, I)$ and integrate the same ODE forward from $t = 0$ to $t = 1$ to obtain generated samples. This is the discretization used in Algorithm 1.

6.6. Training objective. Training is performed using the continuous normalizing flow likelihood objective. Along each trajectory, the log-density evolves according to the instantaneous change-of-variables formula,

$$\frac{d}{dt} \log p_t(x_t) = -\text{div}(v_\theta(t, x_t)).$$

Given a minibatch of data samples $\{x_1^{(j)}\}_{j=1}^B \sim \mu_1$, we integrate each sample backward to obtain a latent point $z^{(j)} = x_0^{(j)}$ and simultaneously accumulate the divergence term. The model log-likelihood is computed as,

$$\log p_\theta(x_1^{(j)}) = \log p_0(z^{(j)}) - \int_0^1 \text{div}(v_\theta(t, x_t^{(j)})) dt,$$

where $p_0 = \mathcal{N}(0, I)$. We minimize the negative log-likelihood,

$$\mathcal{L}_{\text{CNF}}(\theta) = -\frac{1}{B} \sum_{j=1}^B \log p_\theta(x_1^{(j)}).$$

In the low-dimensional synthetic experiments, the divergence is computed exactly using automatic differentiation. The training loss curves for the Gaussian-mixture and torus experiments are shown in Figure 2.

6.7. Optimization. We train using Adam with learning rate 10^{-3} . Gradients are back-propagated through the discretized ODE solver and the accumulated divergence term. We clip the gradient norm at 10 to improve numerical stability. We use a fixed integration horizon $T = 1$, $K = 16$ Runge–Kutta steps during training, and a larger number of steps during sampling for improved sample quality.

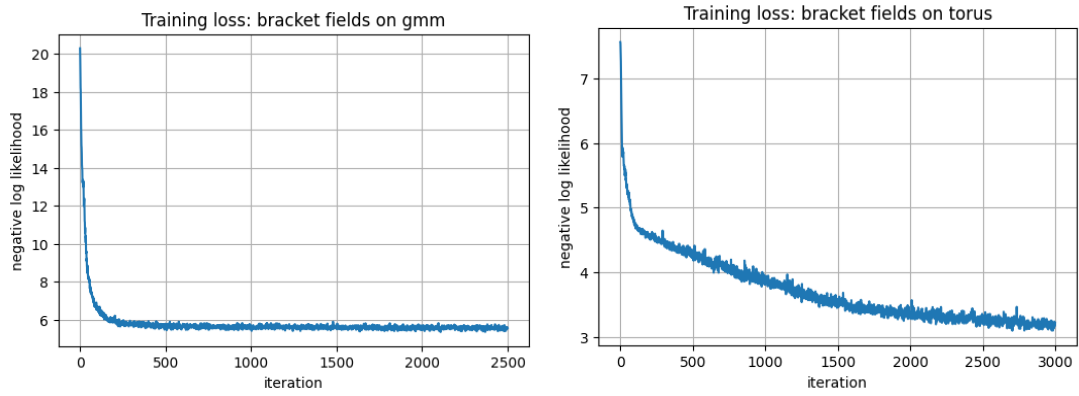


FIGURE 2. Negative log-likelihood training curves for the synthetic Gaussian-mixture and torus experiments.

REFERENCES

- [BMR⁺20] Tom Brown, Benjamin Mann, Nick Ryder, Melanie Subbiah, Jared D Kaplan, Prafulla Dhariwal, Arvind Neelakantan, Pranav Shyam, Girish Sastry, Amanda Askell, et al., *Language models are few-shot learners*, Advances in neural information processing systems **33** (2020), 1877–1901.
- [Cho40] Wei-Liang Chow, *Über systeme von linearen partiellen differentialgleichungen erster ordnung*, Mathematische Annalen **117** (1940), no. 1, 98–105.
- [CRBD18] Ricky TQ Chen, Yulia Rubanova, Jesse Bettencourt, and David K Duvenaud, *Neural ordinary differential equations*, Advances in neural information processing systems **31** (2018).
- [CV25] Marco Caponigro and Arianna Vicari, *Transport maps as flows of control-affine systems*, Journal of Dynamical and Control Systems **31** (2025), no. 3, 23.
- [DSDB16] Laurent Dinh, Jascha Sohl-Dickstein, and Samy Bengio, *Density estimation using real nvp*, arXiv preprint arXiv:1605.08803 (2016).
- [Ela25] Karthik Elamvazhuthi, *Flow matching for measure transport and feedback stabilization of control-affine systems*, arXiv preprint arXiv:2510.02706 (2025).
- [HJA20] Jonathan Ho, Ajay Jain, and Pieter Abbeel, *Denoising diffusion probabilistic models*, Advances in neural information processing systems **33** (2020), 6840–6851.
- [Jur97] Velimir Jurdjevic, *Geometric control theory*, Cambridge university press, 1997.
- [LCBH⁺22] Yaron Lipman, Ricky TQ Chen, Heli Ben-Hamu, Maximilian Nickel, and Matt Le, *Flow matching for generative modeling*, arXiv preprint arXiv:2210.02747 (2022).
- [Mon02] Richard Montgomery, *A tour of subriemannian geometries, their geodesics and applications*, no. 91, American Mathematical Soc., 2002.
- [PNR⁺21] George Papamakarios, Eric Nalisnick, Danilo Jimenez Rezende, Shakir Mohamed, and Balaji Lakshminarayanan, *Normalizing flows for probabilistic modeling and inference*, Journal of Machine Learning Research **22** (2021), no. 57, 1–64.
- [Ras38] Piotr K Rashevsky, *About connecting two points of a completely nonholonomic space by admissible curve*, Uch. Zapiski Ped. Inst. Libknechta **2** (1938), 83–94.
- [SSDK⁺20] Yang Song, Jascha Sohl-Dickstein, Diederik P Kingma, Abhishek Kumar, Stefano Ermon, and Ben Poole, *Score-based generative modeling through stochastic differential equations*, arXiv preprint arXiv:2011.13456 (2020).
- [War83] Frank W Warner, *Foundations of differentiable manifolds and lie groups*, vol. 94, Springer Science & Business Media, 1983.